NANO LETTERS

2009
Vol. 9, No. 4
1506-1510

Method for Suppression of Stacking Faults in Wurtzite III−V Nanowires

Hadas Shtrikman,*,† Ronit Popovitz-Biro,‡ Andrey Kretinin,† Lothar Houben,§ Moty Heiblum,† Małgorzata Bukała,‖ Marta Galicka,‖ Ryszard Buczko,‖ and Perła Kacman‖

Braun Center for Submicron Research, Electron Microscopy Unit, Weizmann Institute, Rehovot, Israel, Institute of Solid State Research, Research Center Jülich, 52425 Jülich, Germany, and Institute of Physics PAS, Al. Lotników 32/46, 02-668 Warsaw, Poland

Received November 20, 2008; Revised Manuscript Received January 13, 2009

ABSTRACT

The growth of wurtzite GaAs and InAs nanowires with diameters of a few tens of nanometers with negligible intermixing of zinc blende stacking is reported. The suppression of the number of stacking faults was obtained by a procedure within the vapor−liquid−solid growth, which exploits the theoretical result that nanowires of small diameter (∼10 nm) adopt purely wurtzite structure and are observed to thicken (via lateral growth) once the axial growth exceeds a certain length.

The interest in one-dimensional structures of III−V compound semiconductors stems from their applicability to studying fundamental physics problems as well as from their potential applications.[1−5] The III−V nanowires (NWs) are commonly nucleated and grown via vapor−liquid−solid (VLS) mechanism with the assistance of metal (usually gold) droplets,[6] which can be applied to any epitaxial growth method such as MOCVD,[7−10] CBE,[11] or molecular beam epitaxy (MBE).[12−16] The diameter and length of the VLS grown NWs are determined by the size of the gold droplets and the duration of the growth, respectively, whereas the shape of NWs is strongly determined by other growth conditions, such as group V/III flux ratio and substrate temperature. Although it was shown that the VLS mechanism allows obtaining NWs uniform in diameter with a large aspect ratio (important features to make them suitable as one-dimensional (1D) conducting channels, waveguides, or nanosize electromechanical systems (NEMS)), controlling the microstructure of such NWs is still a challenging task.

It is widely observed that the crystallographic structure of GaAs, InAs, and some other III−V NWs is strongly dominated by the hexagonal wurtzite (WZ) structure, despite the fact that bulk and two-dimensional growth of these compounds leads to strictly cubic, zincblende (ZB) structure. Moreover, most of such NWs, especially those important for scientific and practical purposes, that is, NWs with diameters of tens of nanometers, embody occasional stacking faults (SFs) originating from the presence of alternating layers of WZ and ZB along the <111> axis, as one can see in the example shown in Figure 1a. Alternatively, a GaAs WZ wire with a significantly lower concentration of SFs is shown in Figure 1b. Even though preliminary evidence indicates that SFs may not be deleterious to electronic conductance,[17] these defects are feared to impede ballistic transport through NWs and are suspected to affect the performance of NWs based optical devices. Therefore, the quest for NWs with a negligible number of SFs has become a major challenge to the growers of 1D III−V semiconductor structures.[18,19] For example, the effect of growth conditions

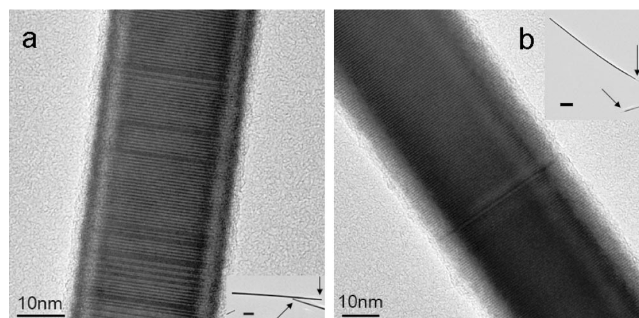

Figure 1. GaAs WZ NWs grown in the [111] direction. (a) Rod shape wire with many SFs grown on a (111)B surface. (b) Pencil shape wire with a single SF grown on a (011) surface. Scale bars are 10 nm. Insets: overview of the NW. Tips are pointed out by arrows. Scale bars are 0.5 μm.

* To whom correspondence should be addressed. E-mail: Hadas.Shtrikman@weizmann.ac.il.
† Braun Center for Submicron Research, Weizmann Institute.
‡ Electron Microscopy Unit, Weizmann Institute.
§ Research Center Jülich.
‖ Institute of Physics PAS.

10.1021/nl803524s CCC: $40.75 © 2009 American Chemical Society
Published on Web 03/02/2009

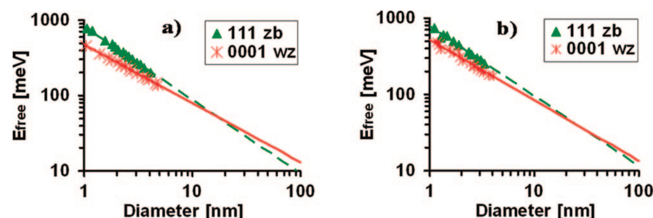

Figure 2. NWs' free energy per atomic pair calculated (symbols) and extrapolated (lines) for InAs (a) and GaAs (b) vs NWs' diameter.

on the occurrence of SFs in both ZB[20] and WZ[21,22] NWs have recently been published.

In this letter we propose a different growth approach of WZ III−V semiconductor NWs along the [0001] direction with a considerably suppressed number of SFs. Although we present mostly GaAs NWs, the obtained results are valid also in the case of InAs.

Our approach is based on combining two findings associated with growth of InAs and GaAs NWs by the VLS method. We combine the theoretical result that NWs of small diameter (∼10 nm) adopt purely WZ structure with the experimental observation that they tend to grow laterally once the axial growth exceeds a certain length. Relating first to the former, we note that lateral surface energy plays a crucial role in the stability of the NWs. The theoretical investigations show[23,24] that the number of dangling bonds at the clean nonsaturated surfaces is larger for ZB than for WZ. This leads to higher lateral surface energy for ZB than for WZ. Thus, the wire's free energy (defined in ref 24 as the total energy of the NW diminished by the energy of bulk crystal, per atomic pair) is lower for WZ structures, which explains the occurrence of the WZ phases during the growth of such NWs. However, contribution of the lateral surface to the total free energy diminishes with increasing the NWs' diameter. For some critical diameter, the inside volume cohesive energy (which in the case of GaAs and InAs, in contrast, is lower for ZB than for WZ) becomes more important, the free energies of the WZ and ZB become comparable and SF are likely to form. The critical diameter is material dependent, and for GaAs numerical estimates in ref 23 give the value of 11.2 nm. Using methods based on the density functional theory to determine the atomic configuration that corresponds to the minimum energy (with full atomic positions relaxation and NW surface reconstruction allowed), we found that for the diameters of up to 5 nm the most stable NWs adopt the WZ (0001) structure.[24] Here, to estimate the free energy for NWs with larger diameter we extrapolate the curves representing the best fit to our results obtained for thin NWs. The extrapolated values of the free energy per atomic pair for ZB and WZ GaAs and for InAs NWs are presented in Figure 2. As shown in the figure, for both GaAs and InAs wires with diameters of the order of 10 nm we obtained the free energy to be still lower for WZ structure, but the energy differences per atomic pair between ZB and WZ are only few millielectron volts, much lower than k_BT at given growth conditions. It should be noted that in the bulk such differences are only 19 meV for GaAs and 14 meV for InAs, and

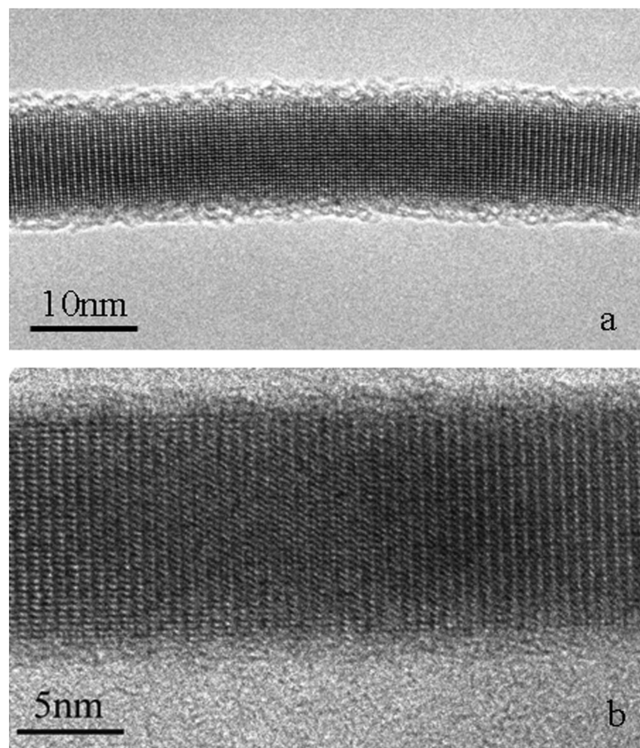

Figure 3. TEM pictures of InAs NW with 10 nm diameter (a) and 13 nm thick GaAs NW (b); no SF are observed.

the ZB structure is still stable below the melting temperature. On the other hand, ZnS, for example, in the energy difference between ZB and WZ phases is as small as 6 meV/pair[25] and is not sufficient to make the compound stable, that is, such energy difference allows for reversible changes from one phase to the other at about 1300 K.[26] These facts suggest that at typical growth temperatures, a difference higher than about 10 meV should lead to NWs with stable structure, but for differences lower by a few millielectron volts the instabilities and SF should appear. For GaAs NWs, we obtained an energy difference between ZB and WZ which is equal to 10.8 and 5.24 meV for 10 and 14 nm thick NWs, respectively. For InAs, the respective differences are 8.06 and 4.37 meV for 10 and 12 nm thick NWs, correspondingly.

In agreement with these theoretical estimates, we indeed observe a diminishing amount of SF with reduction of the wires' diameter. In particular, SF-free InAs wires, as thin as 10 nm or less and 5 μm long, were reproducibly grown. A long fragment of such InAs wire with diameter 10 nm, is shown in Figure 3a. GaAs wires of such thickness are rare but exhibit the same behavior (Figure 3b).[27] It should be noted that although this theory accounts for the most important total energy parameter it does not take into account many other factors, which occur during the growth and influence the NWs crystal structure. In particular, the theory does not account for the nucleation processes that are predominantly determined by the supersaturation, which in turn affects also the alternations between WZ and ZB.[21,22]

The NWs were grown by MBE (in a Riber 32 solid source system) using the VLS method. A layer of gold 0.5−1 nm thick was evaporated directly onto the GaAs substrate (in a

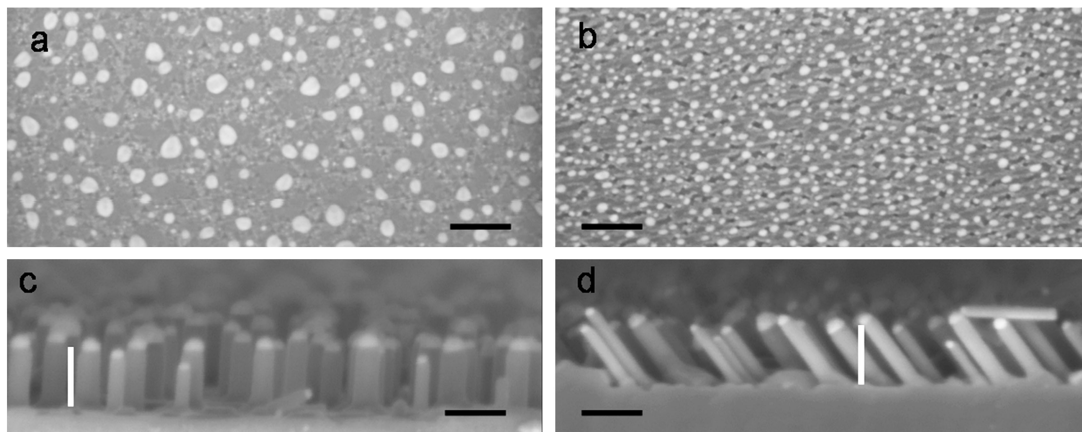

Figure 4. Top: Gold droplets distribution on (111)B GaAs (a) and (011) GaAs (b) after deposition of the same gold thickness and the same annealing conditions. Scale bars are 200 nm. Bottom: short NWs formed after 5 min of growth on (111)B (c) and (011) (d) surfaces. The white bar of the same length on panels c and d illustrates the faster growth on the (011) substrate. Scale bars are 100 nm.

separate chamber attached to the MBE system), after an initial oxide removal at 600 °C. Subsequently, the wafer was moved into the attached MBE growth chamber where GaAs or InAs NWs growth was initiated at a substrate temperature of 550 °C and an As /Ga flux ratio on the order of 200. The analysis of the morphological and structural properties of the wires was performed by SEM (Zeiss Supra 55 system at 2 kV) and TEM (for normal resolution, Philips CM120 microscope operating at 120 kV; for high resolution, FEI Tecnai F30 UT operating at 300 kV). Atomic-resolution high-angle annular dark-field STEM images were taken in a probe-side aberration corrected FEI Titan 80−300 microscope operated at an acceleration voltage of 300 kV. Samples examined by TEM were prepared by dispersing NWs in ethanol using an ultrasonic bath for 1 min, followed by taking a drop from the suspension and placing it on a 300 mesh carbon/collodion /Cu or lacy carbon/Cu grid.

To reduce the number of SF in thicker wires, we take advantage of the tendency of thin wires to grow laterally once the axial growth exceeds a certain mean migration length.[14,28] The idea here is to use the ultrathin, SF free NW as a "core" for further growth into a thicker wire with a tapered/pencil shape morphology. Such shape has previously been related to layer-by-layer growth fed by nucleation of atoms diffusing on the NW sidewalls.[28] Assuming that the thin core NW contains minimal number of SF, the resulting tapered/pencil shape NWs will not have any additional SFs, since no new ones can form in the process of lateral growth. The SFs are not expected to form during the lateral growth because their formation demands moving many atoms, which is energetically very costly. In other words, the energy difference between WZ and ZB phase is too small to compensate for the high energy needed for such a transition. It should be mentioned here that, as shown by Gilles Patriarche et al.,[29] for buried wires such transition is possible. In this case the high energy required for moving the atoms is compensated by energy gain related to adjusting the NW sidewall to the crystallographic structure of the burying layers. However, in our case of free sidewalls, such mechanism is not possible.

Moreover, we note that the crystallographic structure of the laterally grown thicker NW should be WZ, as determined by the structure of the thin WZ core, even in the range where the free energy for the larger final radii is lower in ZB structures. This is due to the fact that, in contrast to the catalytic vertical growth (during which the new atomic layers can easily find positions minimizing the free energy), the lateral growth is rather similar to the noncatalytic layer-by-layer epitaxial growth, where the structure is determined primarily by the substrate. The fact that layers follow the structure of the substrate even for several microns of epitaxial growth was shown by many authors, for example, in ref 30 the growth of a 8.5 μm thick ZB crystalline layer of MnTe (a material having WZ structure under normal conditions) on GaAs (001) substrate was reported.

Apparently, the prerequisite for reproducible growth of such "core"-shell/pencil shape NWs is an ability to control the small dimension of the original gold droplets. Our attempts to obtain small droplets on the commonly used (111)B GaAs surface have shown that in this case it is very difficult to ensure that the droplets will not be overgrown by the bulk growth. However, looking at GaAs NWs grown on the (111)B surface one can observe occasional (very low density) pencil shape NWs among a high density of rod shape wires. This is due to the typical distribution of gold clusters on a (111)B surface, as shown in Figure 4a. Among the uniformly distributed large gold clusters with diameters ~50 nm, occasional small 10−20 nm diameter droplets are observed. In contrast to the (111)B surface, the distribution of gold clusters on the (011) surface (formed under the same conditions) is very different as can be seen in Figure 4b. Here the gold clusters are typically much smaller (10−20 nm) and quite uniform in size.

Images of the top and side views of fully grown pencil shape GaAs NWs on a (011) surface are seen in Figure 5. As one can see in the figure, on the (011) surface we obtain a much larger population of such wires as compared to the (111)B surface.

Detailed STEM studies performed on pencil shape wires show (Figure 6) that they have a perfect WZ structure with

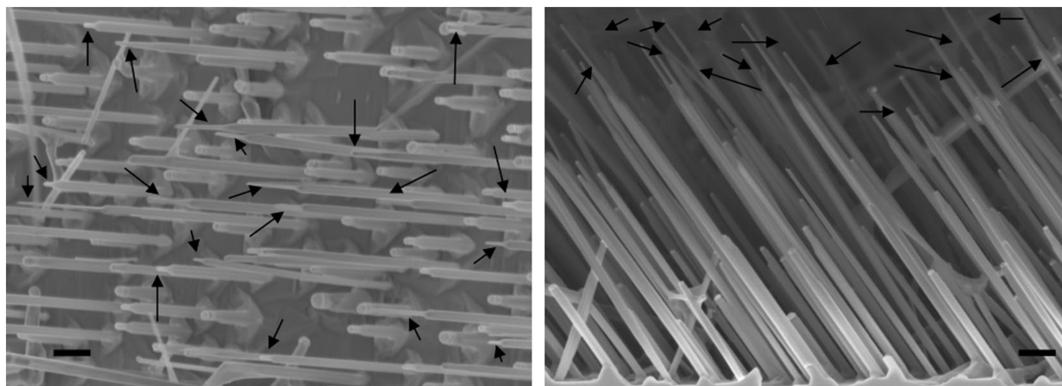

Figure 5. SEM of GaAs NW on (011) surface. Top view (left) and side view (right): both are showing a high concentration of pencil shape NWs some of them pointed out with arrows. Scale bars are 200 nm.

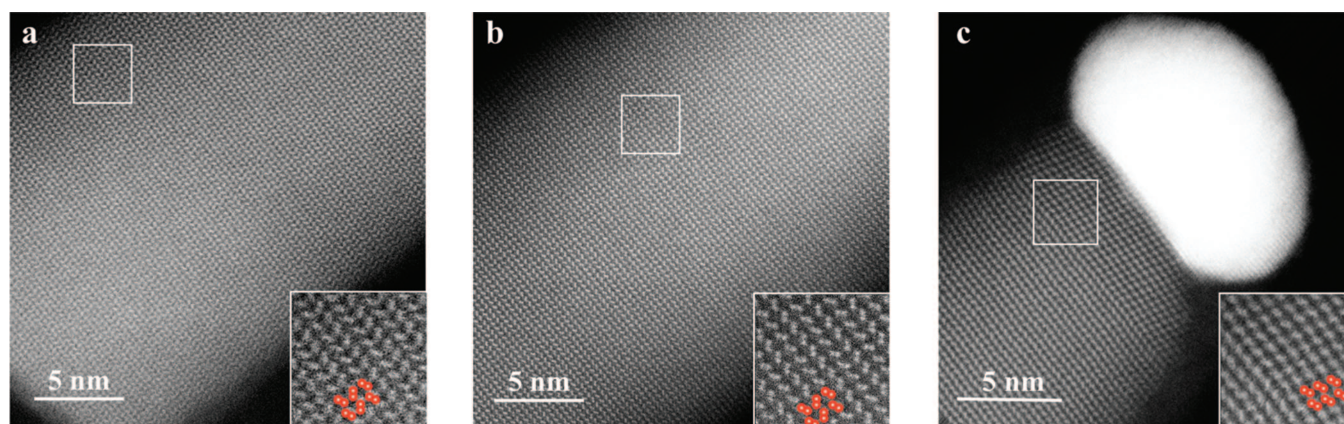

Figure 6. High-angle annular dark-field STEM image of a pencil shape GaAs NW, grown on a (011) surface, showing no SF along the wire: at the bottom of the NW (a), in the center (b) and at the tip (c). A transition from WZ to ZB is depicted in panel c. Insets show the lattice structure in the magnified region.

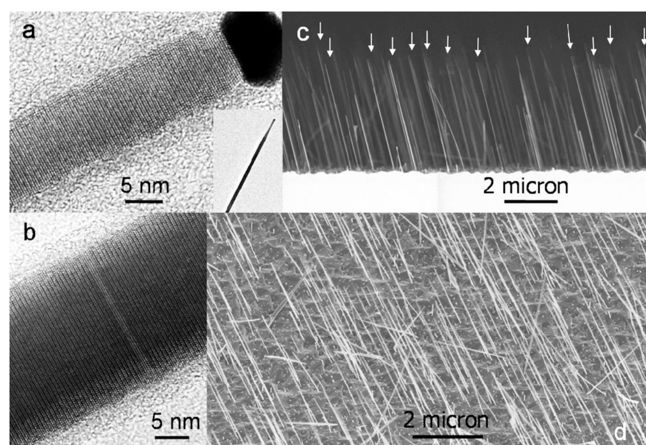

Figure 7. GaAs NWs grown on a (211)B surface. (a,b) TEM images taken from the tip and the center of a single pencil shape wire. Inset: low magnification image of single wire. (c,d) SEM images of the as-grown sample taken from the side and at 45°, respectively. (Some of the pencil shape wires are marked with arrows).

no visible SF, except for a change to ZB structure adjacent the tip (resulting from closing the shutters).

Trying to understand the above results, we note that the wetting/adhesion properties of gold can be related to the typical density of dangling bonds covering the surface of the substrate. Namely, higher density of dangling bonds would lead to stronger adhesion to the surface (due to energy gain upon passivation of the dangling bonds). In turn, stronger adhesion translates to lower mobility of gold atoms on the surface, restraining the aggregation that takes place in Oswald Ripening like processes. In other words, a lower surface mobility prevents the small gold droplets, which are initially formed upon heating, from joining together into larger droplets, as we have seen on the (111) surface. Consequently, since the density of dangling bonds at the (011) surface of ZB is higher than at the (111) surface and the density of bonds at the (211) surface is expected to be even higher than that,[31] we decide to use the latter for the growth of a high density of pencil shape NWs. Indeed, on

Table 1. Comparison between Growth of GaAs NW on the (111)B, (011), and (211)B Surfaces

substrate	nanowire structure	average reclining angle (degrees)	maximum length (μm)	total number of stacking faults	number of wires measured
(111)B	WZ	90	3.0	many	25
(011)	WZ	55	5.0	0−12	20
(211)B	WZ	73	4.0	1−10	22

the (211)B substrate we managed to grow pencil shape GaAs NWs, which nucleated around a very thin core of ∼10 nm (Figure 7a). In this growth, we used a particularly thin layer of gold, some 0.3 nm thick. A gold layer of such thickness on a (111)B substrate becomes completely covered by the bulk growth and thus is unable to initiate growth of NWs. On the (211)B surface, in spite of the very small diameter of gold droplets, wires emerge (at an angle of about 73 degrees, i.e., they grow in the most energetically favorable direction, along the [0001] crystallographic axis). Figure 7c,d show the general appearance of an as grown sample of GaAs nanowires on a (211)B surface. The TEM studies of some of these wires confirm that they indeed exhibit a significantly lower concentration of SF than seen in wires growing on the (111)B surface (see Figure 7b).

Finally, we note that the axial growth of thin wires from small droplets not only ensures a suppressed concentration of SF but also provides an enhanced growth rate as compared to the growth of the comparable rod shape wires, thanks to the fact that thin wires grow faster.[12] This is further subjected to the effect of the tilt angle that increases the direct impingement of atoms on the wires' sidewalls.[32] Consequently, the NWs that form after lateral growth are longer from the respective rod shape NWs by at least 30%. The smaller average droplet size as well as the reclining angle, which facilitates collection of more of the impinging atoms, are most likely responsible for the fact that the growth on (011) surface produces, after five minutes of growth under similar conditions, wires which are about 20% longer than wires grown on (111)B surface. Some typical characteristics of the NWs grown in the [0001] direction on the three different substrate orientations are given in Table 1.

In conclusion, being equipped with the theoretical understanding and supported by the experimental finding that thin wires on the order of 10 nm are bound to be WZ and free of SF, we suggest that such wires can be used as a core for further growth of thicker wires with a tapered/pencil shape morphology. In as much as SFs can form only along the [0001] axis, in principle the lateral expansion of NWs growing in the [0001] direction cannot introduce any new SF; the lattice structure is dictated already during the growth of the "core". We have shown that by such procedure WZ III−V NWs as thick as a few tens of nanometers with considerably reduced number of SF can be grown.

Acknowledgment. The Warsaw group thanks EC network SemiSpinNet (PITN-GA-2008-215368) for support. All computations were carried out in CI TASK in Gdansk. The transmission electron microscopy studies were conducted at the Irving and Cherna Moskowitz Center for Nano and Bio-Nano Imaging at the Weizmann Institute of Science. The access to the high-resolution STEM instrumentation was provided by the Ernst-Ruska Centre for Microscopy and Spectroscopy with Electrons of the Research Centre Jülich. H.S. acknowledges fruitful discussions with Dr. Brent Wacaser.

References

(1) Bryllert, T.; Wernersson, L.-E.; Fröberg, L.; Samuelson, L. *IEEE-Electron Device Lett.* **2006**, *27*, 323.
(2) Huang, Y.; Duan, X. F.; Wei, Q.; Lieber, C. M. *Science* **2001**, *291*, 630.
(3) Thelander, C.; Mårtensson, T.; Björk, M. T.; Ohlsson, B. J.; Larsson, M. W.; Wallenberg, L. R.; Samuelson, L. *Appl. Phys. Lett.* **2003**, *83*, 2052.
(4) Li, Y.; Qian, F.; Xiang, J.; Lieber, C. M. *Mater. Today* **2006**, *9*, 18.
(5) Hiruma, K.; Yazawa, M.; Haraguchi, K.; Ogawa, K.; Katsuyama, T.; Koguchi, M.; Kakibayashi, H. *J. Appl. Phys.* **1993**, *74*, 3162.
(6) Wagner, R. S.; Ellis, W. C. *Appl. Phys. Lett.* **1964**, *4*, 189.
(7) Krishnamachari, U. M.; Borgstrom, M.; Ohlsson, B. J.; Panec, N.; Samuelson, L.; Seifert, W.; Larsson, M. W.; Wallenberg, L. R. *Appl. Phys. Lett.* **2004**, *85*, 2077.
(8) Koguchi, M.; Kakibayashi, H.; Yazawa, M.; Hiruma, K.; Katsuyama, T. *Jpn. J. Appl. Phys.* **1992**, *31*, 2061.
(9) Bauer, J.; Gottschalch, V.; Paetzelt, H.; Wagner, G.; Fuhrmann, B.; Leipner, H. S. *J. Cryst. Growth* **2006**, *298*, 625.
(10) Dayeh, S. A.; Yu, E. T.; Wang, D. *Nano Lett.* **2007**, *7*, 2486.
(11) Persson, A. I.; Ohlsson, B. J.; Jeppesen, S.; Samuelson, L. *J. Cryst. Growth* **2004**, *272*, 167.
(12) Dubrovskii, V. G.; Cirlin, G. E.; Soshnikov, I. P.; Tonkikh, A. A.; Sibirev, N. V.; Samosenko, Y. B.; Ustinov, V. M. *Phys. Rev. B* **2005**, *71*, 205325.
(13) Harmand, J. C.; Tchernycheva, M.; Patriarche, G.; Travers, L.; Glas, F.; Cirlin, G. *J. Cryst. Growth* **2007**, *301*, 853.
(14) Tchernycheva, M.; Travers, L.; Patriarche, G.; Glas, F.; Harmand, J.-C.; Cirlin, G. E.; Dubrovskii, V. G. *J. Appl. Phys.* **2007**, *102*, 094313.
(15) Fontcuberta i Moral, A.; Colombo, C.; Abstreiter, G.; Arbiol, J.; Morante, J. R. *Appl. Phys. Lett.* **2008**, *92*, 063112.
(16) Wu, Z. H.; Gierak, J.; Bourhis, E.; Biance, A. L.; Ruda, H. E. *Proc. SPIE* **2005**, *5971*, 597117.
(17) Pfund, A.; Shorubalko, I.; Leturcq, R.; Borgströmb, M. T.; Gramm, F.; Müller, E.; Ensslin, K. *Chimia* **2006**, *60*, 729.
(18) Joyce, H. J.; Gao, Q.; Tan, H. H.; Jagadish, C.; Kim, Y.; Fickenscher, M. A.; Perera, S.; Hoang, T. B.; Smith, L. M.; Jackson, H. E.; Yarrison-Rice, J. M.; Zhang, X.; Zou, J. *Adv. Funct. Mater.* **2008**, *18*, 3794.
(19) Cornet, D. M.; Mazzetti, V. G. M.; LaPierre, R. R. *Appl. Phys. Lett.* **2007**, *90*, 013116.
(20) Shtrikman, H.; Popovitz-Biro, R.; Kretinin, A.; Heiblum, M. *Nano Lett.* **2009** *9*, 215.
(21) Plante, M. C.; LaPierre, R. R. *Nanotechnology* **2008**, *19*, 495603.
(22) Plante, M. C.; LaPierre, R. R. *J. Cryst. Growth* **2008**, *310*, 356.
(23) Akiyama, T.; Sano, K.; Nakamura, K.; Ito, T. *Jpn. J. Appl. Phys.* **2006**, *45*, L275.
(24) Galicka, M.; Bukała, M.; Buczko, R.; Kacman, P. *J. Phys.: Condens. Matter* **2008**, *20*, 454226.
(25) Yeh, C.-Y.; Lu, Z. W.; Froyen, S.; Zunger, A. *Phys. Rev. B* **1992**, *46*, 10086.
(26) Rumayantsev, Y. M.; Kuznetsov, F. A.; Stroitelve, S. A. *Kristallografiya* **1965**, *10*, 263.
(27) Bukała, M.; Galicka, M.; Buczko, R.; Kacman, P.; Shtrikman, H.; Popovitz-Biro, R.; Kretinin, A.; Heiblum, M. AIP Conference Proceedings Series, ICPS 29, Rio de Janeiro, Brazil, 2008 (to be published on-line).
(28) Chen, C.; Plante, M. C.; Fradin, C.; LaPierre, R. R. *J. Mater. Res.* **2006**, *21*, 2801.
(29) Patriarche, G.; Glas, F.; Tchernycheva, M.; Sartel, C.; Largeau, L.; Harmand, J. C.; Cirlin, G. E. *Nano Lett.* **2008**, *8*, 1638.
(30) Janik, E.; Dynowska, E.; Bak-Misiuk, J.; Szuszkiewicz, W.; Wojtowicz, T.; Karczewski, G.; Zakrzewski, A. K.; Kossut, J. *Thin Solid Films* **1995**, *267*, 74.
(31) Ding, Y.; Wang, Z. L.; Sun, T.; Qiu, J. *Appl. Phys. Lett.* **2007**, *90*, 153510.
(32) Dubrovskii, V. G.; Sibirev, N. V.; Cirlin, G. E.; Tchernycheva, M.; Harmand, J. C.; Ustinov, V. M. *Phys Rev. E* **2008**, *77*, 031606.

NL803524S